

Mechanism of formation of nanocrystalline particles with core-shell structure based on titanium oxynitrides with nickel in the process of plasma-chemical synthesis of TiNi in a low-temperature nitrogen plasma

Yuliya A. Avdeeva^a, Irina V. Luzhkova^b, Alexey N. Ermakov^c

Institute of Solid State Chemistry, Ural Branch, Russian Academy of Sciences, Ekaterinburg, 620990, Russia

^ay-avdeeva@list.ru, ^bkey703@yandex.ru, ^cermakovihim@yandex.ru

Corresponding author: Yu. A. Avdeeva, y-avdeeva@list.ru

PACS 61.46.+w, 61.46.-w, 61.66.Fn

ABSTRACT This paper presents the results of experiments, structural and morphological certification and modeling of ultrafine and nanocrystalline TiN-Ni “core-shell” structures obtained during plasma-chemical synthesis of industrially manufactured microcrystalline TiNi. Experiments on plasma-chemical synthesis were carried out by recondensation of ultrafine and nanocrystalline powders in a rotating cylinder of gaseous nitrogen. X-ray phase analysis and high-resolution transmission electron microscopy (HR TEM) showed the presence of refractory titanium compounds with nitrogen and metallic nickel, which are part of the core-shell structures, including the metastable, highly deformed complex nitride $Ti_{0.7}Ni_{0.3}N$ of hexagonal modification. HR TEM studies showed the localization of phases determined by X-ray diffraction and confirmed the “core-shell” structure on the example of nanocrystalline TiN-Ni fraction. Based on the experimental results, we have developed a model of crystallization of TiN-Ni “core-shell” structures under the conditions of a rotating cylinder of gaseous nitrogen, where the crystallization rate is 10^5 °C/s.

KEYWORDS titanium nickelide, nickel, plasma-chemical synthesis, low-temperature plasma, X-ray phase analysis, high-resolution transmission electron microscopy.

ACKNOWLEDGEMENTS The work was carried out in accordance with the state assignment for the Institute of Solid State Chemistry of the Ural Branch of the Russian Academy of Sciences (theme No 0397-2019-0003 “New functional materials for promising technologies: synthesis, properties, spectroscopy and computer simulation”).

FOR CITATION Avdeeva Yu.A., Luzhkova I.V., Ermakov A.N. Mechanism of formation of nanocrystalline particles with core-shell structure based on titanium oxynitrides with nickel in the process of plasma-chemical synthesis of TiNi in a low-temperature nitrogen plasma. *Nanosystems: Phys. Chem. Math.*, 2022, **13** (2), 212–219.

1. Introduction

Refractory compounds of titanium in the form of carbides and nitrides find wide application in different fields of technology. They are extensively used as tool and construction materials, as well as coatings for various purposes [1–5]. Another area of application of refractory compounds, including ultrafine and nanocrystalline compounds of all elements of subgroup IV-VIA of the Periodic system, is their use as modifying additives in foundry production, improving the final physical and mechanical properties of products [6, 7]. Various methods for the formation of ultrafine and nanocrystalline compounds of both titanium nitride and titanium carbide are amply covered in the literature [8–10]. It should be noted that all methods differ not only in the instrumentation involved in the preparation of dispersed refractory materials and compounds, but also in the productivity, which immediately affects the applicability of various synthesis methods, including their applicability under production conditions. Besides, an important aspect of the formation of refractory compounds can be the possibility of coating of particles, including ultra- or nanodispersed ones, with individual metals or their intermetallic compounds. The implementation of such ideas is considered in a number of publications [11–15], and the works of B. Chalmers (see, for example, [16]) provide a theoretical basis for heterogeneous nucleation, which makes it possible to form “core-shell” structures, where refractory compounds will act as a core, and the metal phases – as a shell of nanocrystalline particles.

The most convenient method for the formation of nanocrystalline particles based on refractory compounds with a “core-shell” structure, in which metal components participate, is extreme effect on microcrystalline materials, characterized by high rates of evaporation and crystallization. One of such methods is plasma-chemical synthesis in low-temperature nitrogen plasma with subsequent crystallization in a rotating cylinder of gaseous nitrogen. Methods of plasma-chemical synthesis suitable for the formation of a large number of ultra- and nanodispersed materials are quite

widely described in the literature [17, 18]. In particular, the final composition of synthesis products depends on the chemical composition of feedstock, processing conditions, gaseous media used for plasma formation processes, cooling, and transportation, as well as on the consideration of the issues of pyrophoricity reduction.

In this paper, to obtain ultrafine and nanocrystalline TiN-Ni powder materials, we proposed to use plasma-chemical synthesis in a low-temperature nitrogen plasma, which, in accordance with [19], makes it possible to obtain “core-shell” structures from microcrystalline powders of commercially produced titanium nickelide under “quasi-equilibrium” conditions. The main goal of the presented work is to form the scientific basis for obtaining ultrafine and nanocrystalline compositions in the form of TiN-Ni core-shell structures under the conditions of plasma-chemical synthesis in a low-temperature (4000–6000°C) nitrogen plasma.

2. Methods

In this work, to obtain ultra- and nanodispersed TiN-Ni “core-shell” structures, the method of plasma-chemical synthesis was used, followed by recondensation of titanium nickelide TiNi evaporated to the atomic state in a rotating cylinder of gaseous nitrogen. The crystallization rate under these conditions was 10^5 °C/s. Microcrystalline (~ 40 μm) titanium nickelide PN55T45 produced by OAO Polema (Tula) was used as the initial precursor raw material. After recondensation, the mixture of ultrafine and nanocrystalline synthesis products was transported to classifier 1, a vortex-type cyclone, and classifier 2, a bag-type fabric filter, where separation into ultrafine and nanocrystalline fractions of powder media was carried out. Each of the obtained fractions was encapsulated in a mixture of gasoline vapors and organic components to reduce the pyrophoricity of fine powders, which allows the resulting compositions to be stored under normal conditions. The technique of plasma-chemical synthesis according to the plasma recondensation scheme is best documented in [20].

The recondensed products of plasma-chemical synthesis were studied by X-ray phase analysis (SHIMADZU XRD – 7000 CuK α -cathode X-ray diffractometer) and high-resolution transmission electron microscopy (JEOL JEM 2100 transmission electron microscope). The results of instrumental studies were processed using modern software, so the X-ray data were processed in WinXPOW software packages (compatible with the ICDD database), and PowderCell 2.3 (refining of unit cell parameters). Electron microscopic images were processed in the DigitalMicrograph 7.0 software in order to analyze profilograms and fast Fourier transform, which confirms the radiography data.

The ultrafine fraction was studied by scanning tunneling microscopy on an SMM 2000 T tunneling microscope (Zelenograd, Moscow region).

3. Results and discussion

Refractory compounds of titanium with carbon and nitrogen crystallize, as a rule, in the form of cubic face-centered lattices of the NaCl type. In addition to individual carbides and nitrides, in the presence of both carbon and nitrogen simultaneously, refractory titanium compounds can be formed during synthesis, including those with the participation of oxygen, whose lattices are isomorphic to the NaCl structure.

The results of X-ray studies of the ultrafine fraction from the cyclone and the nanocrystalline fraction from the filter are shown in Fig. 1 and Table 1. So, the ultrafine fraction of the recondensed TiNi from the cyclone (Table 1, experiment 1) is represented by a mixture of refractory interstitial phases in the form of TiC $_x$ N $_y$ ($x + y \leq 1$) and cubic titanium nitride TiN (sp. gr. Fm-3m). Nickel, in its turn, is redistributed between the individual cubic modification (sp. gr. Fm-3m) [21] and the complex nitride Ti $_{0.7}$ Ni $_{0.3}$ N of the hexagonal modification (sp. gr. P-6m2) [22], being, in accordance with [23], in a highly deformed state along the (101) direction, which is expressed by the presence of a single reflection on the X-ray diffraction pattern. Additionally (Fig. 1, Table 1, experiment 1), there are reflections of cubic solid solutions of isomorphic TiN and intermetallic compounds of the Ti–Ni system: nickelide TiNi (sp. gr. Pm-3m) [24] and hexagonal TiNi $_3$ (sp. gr. P6 $_3$ /mmc) [25].

The nanocrystalline fraction of recondensed titanium nickelide extracted from the bag-type filter is represented by nonstoichiometric cubic titanium nitride TiN $_y$ (sp. gr. Fm-3m), cubic Ni (sp. gr. Fm-3m) [21] and complex nitride Ti $_{0.7}$ Ni $_{0.3}$ N of hexagonal modification (sp. gr. P-6m2) [22], which is also in a highly deformed state. The presence of a small amount of cubic carbonitride TiC $_x$ N $_y$ ($x + y \leq 1$) in the fraction from the vortex-type cyclone may be due to the fact that preliminary cleaning of the plasma-chemical installation before the experiment was carried out with powdered titanium carbide TiC.

Based on the data of X-ray phase analysis it should be noted that although the temperature of plasma-chemical synthesis (4000–6000°C) exceeds considerably the melting and boiling temperatures of Ti-Ni intermetallic phases, the TiNi and TiNi $_3$ intermetallics are present in the recondensed fraction from the vortex-type cyclone (Table 1, experiment 1). This can be justified by both the high flow rate of vortex plasma in the plasma-chemical reactor (~ 55 m/s) and the non-equilibrium of the plasma itself. As regards the disperse composition, it should be noted that the fraction from the cyclone is much larger and it contains inclusions of spherical shape. This is due to crystallization according to the “vapor-liquid-solid” scheme providing rounded surfaces of nanocrystalline particles.

Following the description of the X-ray data, special attention should be given to a considerable content of cubic nickel metal determined from the data of semi-quantitative analysis. In particular, it should be pointed out that nickel is a

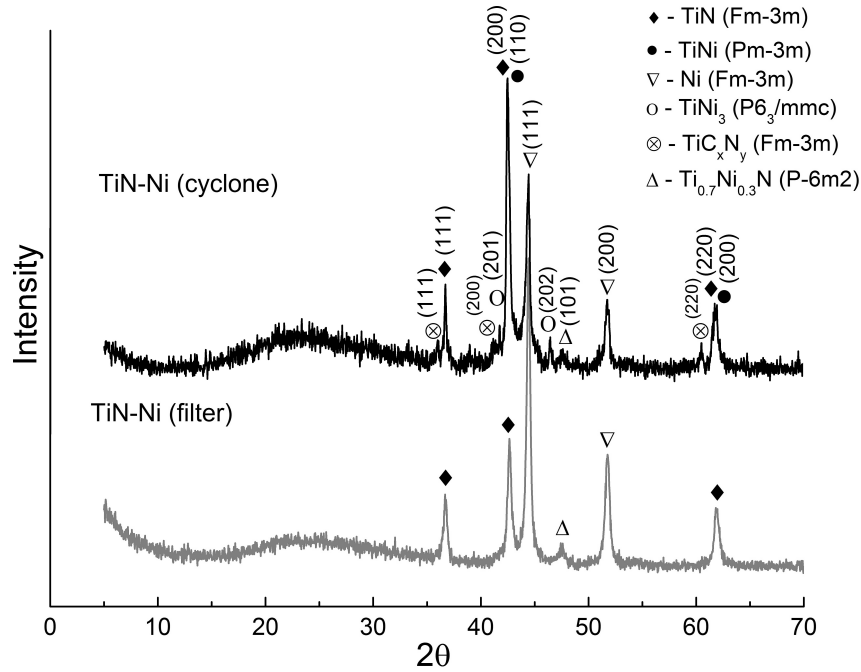


FIG. 1. X-ray patterns of TiN-Ni fractions after plasma-chemical synthesis

TABLE 1. Phase composition and lattice parameters of TiN-Ni fractions after plasma-chemical synthesis

Fraction	Phase composition (± 2 wt%), a, b, c (± 0.0001 Å)	$S_{sp}, m^2/g$	$\rho, g/cm^3$	d, μm
Cyclone	TiC _x N _y (Fm-3m), (24%), a = 4.3138	14.3	6.4	0.065
	TiN _y (Fm-3m), (2%), a = 4.2329			
	Ni (Fm-3m), (19%), a = 3.5234			
	TiNi (Pm-3m) (17%), a = 2.9986			
	TiNi ₃ (P6 ₃ /mmc) (38%), a = 5.0658, c = 8.4040			
	Ti _{0.7} Ni _{0.3} N (P-6m2) – not calculated			
Filter	TiN _y (Fm-3m), (53%), a = 4.2330	33.9	6.5	0.027
	Ni (Fm-3m), (43%), a = 3.5274			
	Ti _{0.7} Ni _{0.3} N (P-6m2), (3%), a = 2.9348, c = 2.8996			

material for selective filter of CuK α emission [26], which contributes to a decrease in the intensity of all determined phase components except for nickel itself. At the same time, when comparing the evaporation and crystallization temperatures of nickel and other X-ray fixed phase components, it can be assumed that the metal shell completely covers ultra- and nanodispersed particles based on refractory titanium compounds giving rise to a “core-shell” structure. However, if we are guided by the observance of the Arrhenius law and, accordingly, the “quasi-equilibrium” of processes [19] occurring under conditions of a hardening chamber, it must be stated that complete titanium nitrides are hardly wetted with nickel melts, and the wetting angle in this case is 120° [27]. In [27], it is reported that in the case of nonstoichiometric titanium nitride (\sim TiN_{0.7}), the angle of wetting with nickel melt decreases to 3°, which provides coating of ultra- and nanodispersed particles based on titanium nitride with nickel.

The visualization of the formed “core-shell” structures was demonstrated by HR TEM and scanning tunneling microscopy of recondensed titanium nickelide fractions from a cyclone (Fig. 2a) and a bag-type filter (Fig. 2b,c). Figures 2a,b present the total sets of particles, whose average size determined from direct measurements is, in accordance with the distribution histogram (Fig. 2d), 63 nm for the fraction from the cyclone and 20 nm for the fraction from the filter.

The magnification of individual particles from the filter shown in Fig. 3 allows one to see a multilayer structure of nanocrystalline particles, in which a layer of metallic nickel is presented as a high-contrast shell and the dark core is

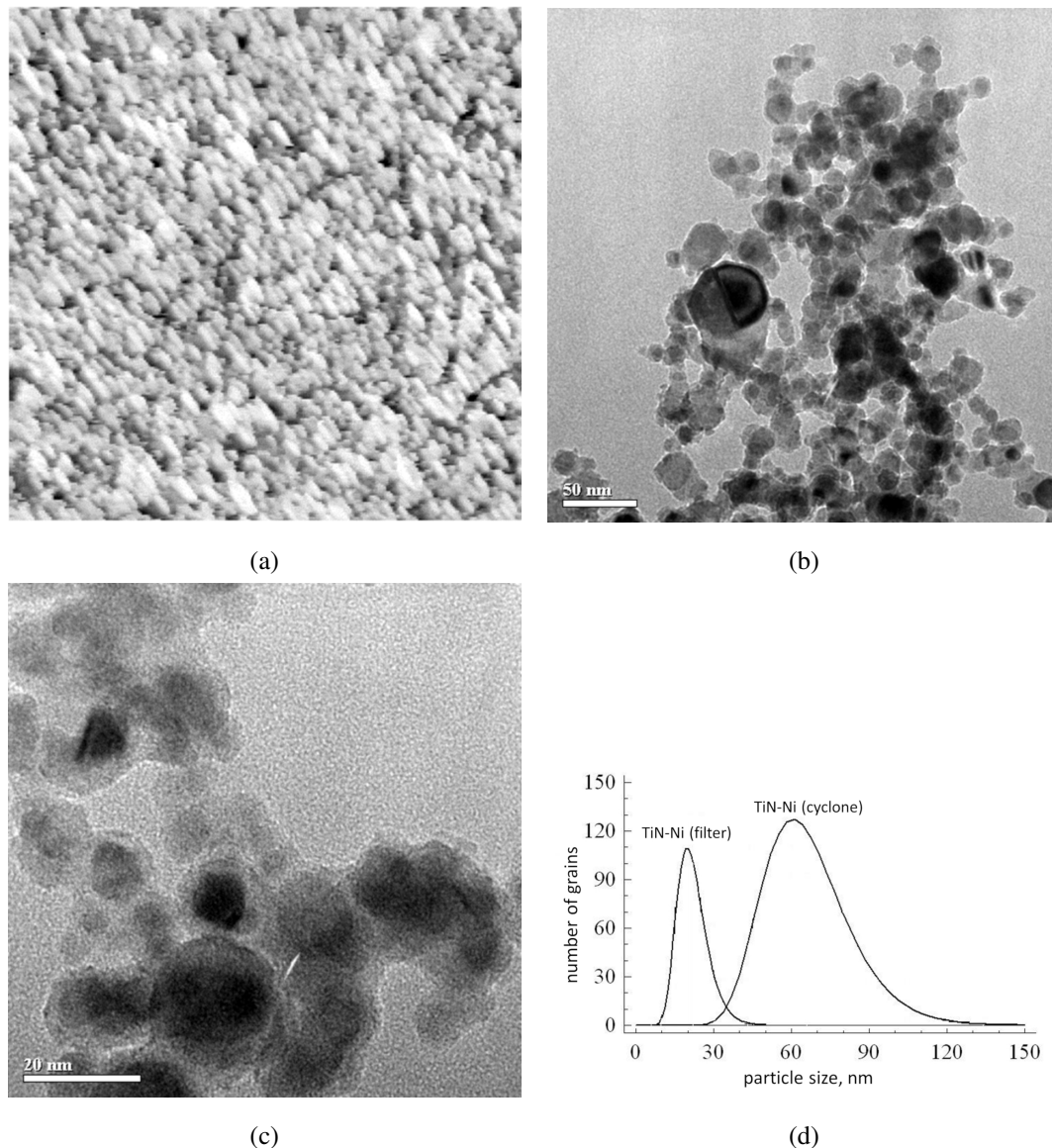


FIG. 2. Results of scanning tunneling and transmission microscopy of ultra- and nanodispersed TiN-Ni powders: a – STM fraction from the cyclone, scan size $2.8 \mu\text{m} \times 2.8 \mu\text{m} \times 87.07 \text{ nm}$, b, c – HR TEM fraction from the filter, d – particle size distribution histograms

composed of refractory interstitial phases recorded by X-ray diffraction. The maximum resolution images of individual sections (Fig. 3-6), containing nanocrystalline particles with a “core-shell” structure made it possible to interpret the individual phase components based on the measurement data of interplanar distances. In particular, in accordance with the measurements of interplanar distances (Fig. 3) and their comparison with the ICDD data, it was found that a layer of hexagonal Ni metal (sp. gr. $P6_3/mmc$) is formed on the surface of nanocrystalline particles [28]. Fig. 4a [29] shows a nanocrystalline particle, in which, according to the measurements of interplanar distances, a transition from metallic nickel to its oxide Ni_2O_3 is observed, which, in turn, is transformed into the complex nitride $\text{Ti}_{0.7}\text{Ni}_{0.3}\text{N}$. Fig. 4b shows monoclinic TiNi and tetragonal titanium nitride Ti_2N . Fig. 4c illustrates a nanoparticle whose shape is close to hexagonal, and the phase composition, according to the measurements of interplanar distances, is represented by the Ti_3Ni_4 intermetallic phase of rhombohedral modification.

In continuation of the description of electron microscopic studies, it should be noted that in the nanocrystalline fraction from the filter of recondensed titanium nickelide it was not possible to display and interpret the planes of refractory compounds based on titanium oxynitride $\text{TiN}_{0.84}\text{O}_{0.11}$ or other refractory phases. At the same time, considering that the X-ray phase analysis technique has a volumetric character compared to the capabilities of transmission electron microscopy characterized by high locality, the X-ray diffraction and HR TEM data complement each other. Thus, the refractory base in the form of $\text{TiN}_{0.84}\text{O}_{0.11}$ oxynitride can be considered as a refractory core of the “core-shell” structure,

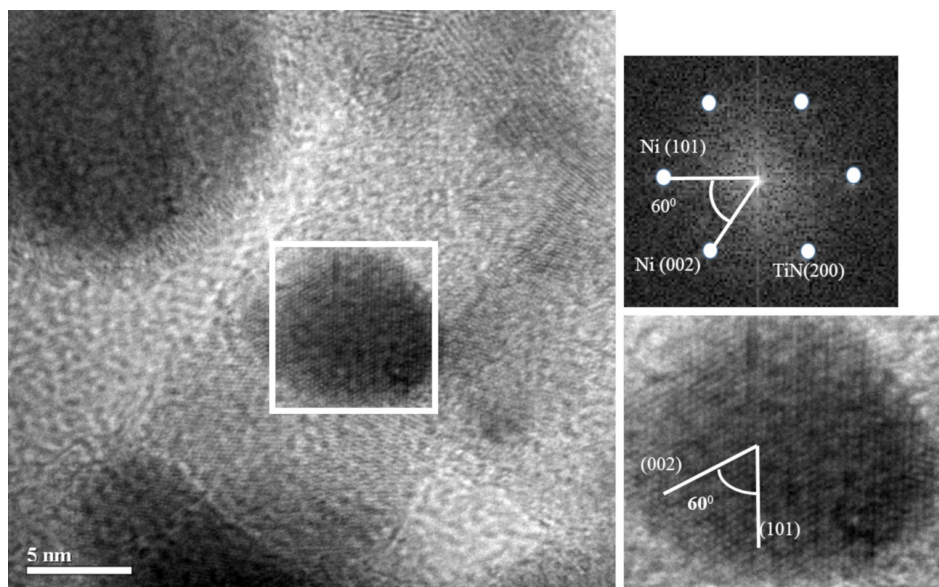


FIG. 3. HR TEM image of a segment of the fraction from TiN-Ni filter

where the peripheral layers can be represented by both locally positioned intermetallic compounds of the Ti-Ni system and bulk phases $\text{Ti}_{0.7}\text{Ni}_{0.3}\text{N}$ and Ni reflected by X-ray.

On the basis of the performed studies, it is possible to develop a model of phase formation of a “core-shell” structure in the process of crystallization of evaporated titanium nickelide in a rotating cylinder of gaseous nitrogen taking place in a quenching chamber.

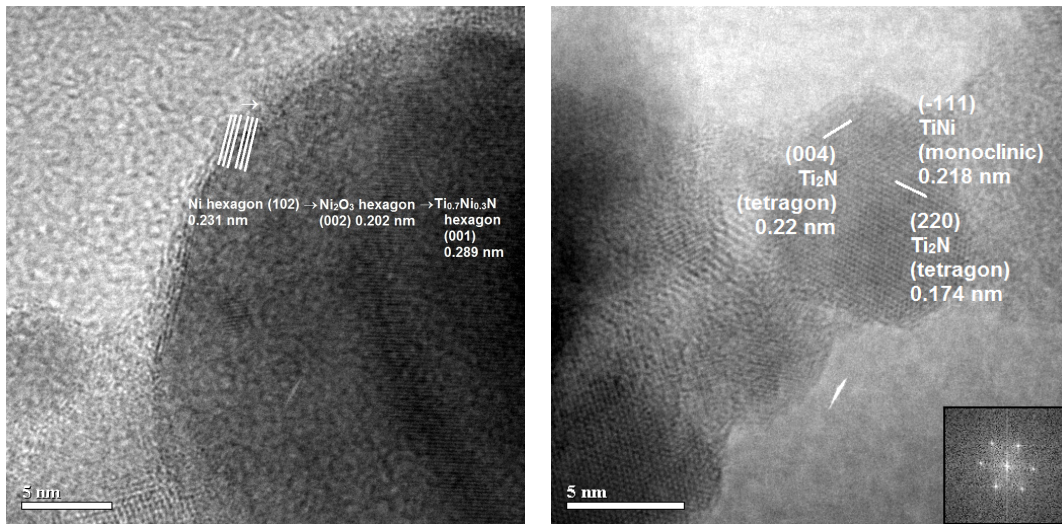
The model of TiN-Ni “core-shell” structure formation during plasma-chemical synthesis of TiNi can be substantiated in terms of physicochemistry by comparing the functions $\Delta G(T)$ (Fig. 5) [30] for all phase components (TiC, TiN, TiNi, TiNi_3) determined radiographically, except for $\text{Ti}_{0.7}\text{Ni}_{0.3}\text{N}$ and Ni, since for the former component there is no available information, while for individual metals $\Delta G(T) = 0$. It can be seen from the graphs that intermetallic phases of titanium with nickel exist at $\Delta G(T)$ values closer to 0 compared with refractory titanium-containing phase components at identical temperatures. At the same time, Ti-Ni intermetallic phases have relatively low melting points compared with refractory titanium carbide-nitride compounds.

In the process of modeling of the recondensed “core-shell” structures, the quenching chamber is separated by temperature barriers, for which the crystallization temperatures of the phase components recorded in the process of X-ray phase analysis are used, see Table 2. Note also that in the modeling process account is taken of the boiling points of both refractory components and individual metals, on the basis of which the individual components of ultra- and nanodispersed “core-shell” structures are formed.

TABLE 2. Melting and boiling points of phase components in the TiN-Ni system

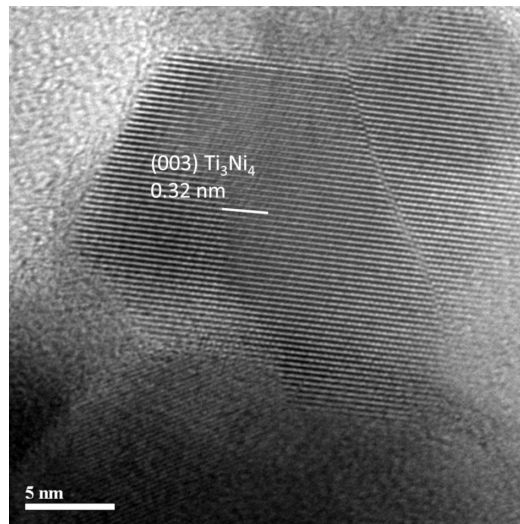
Component	$T_{melt}, ^\circ\text{C}$	$T_{boil}, ^\circ\text{C}$
TiN	2900	–
Ni	1453	2900
TiNi	1310	–

Considering that the low-temperature plasma in the performed experiments corresponded to the temperature range 4000–6000°C, the first temperature barrier can correspond to 4000°C as the lower threshold value of cold plasma. Since the melting temperature of the initial raw material, titanium nickelide, is equal to 1310°C [31], under low-temperature plasma conditions, it is in the state of two metals, Ti and Ni, evaporated to atomic level. It should be noted that the plasma-chemical installation was cleaned with titanium carbide TiC, the trace amounts of which could remain in the plasma-chemical reactor. At 3300°C, the TiC_{1-x} carbide phase and the highly defective TiN_{1-y} titanium nitride phase newly formed from atomic titanium and nitrogen crystallize from the vapor phase [32–35]. Thus, two types of particles crystallize under the conditions of the quenching chamber. Particles of the first type are formed on the basis of titanium carbonitride TiC_xN_y ($x + y \leq 1$) when passing the first temperature barrier under nitrogen atmosphere. Particles of the second type are formed at 2900°C, which corresponds to the crystallization of titanium nitride TiN [36]. The



(a)

(b)



(c)

FIG. 4. HR TEM of particles in the TiN-Ni fraction (a, b, c) from the filter

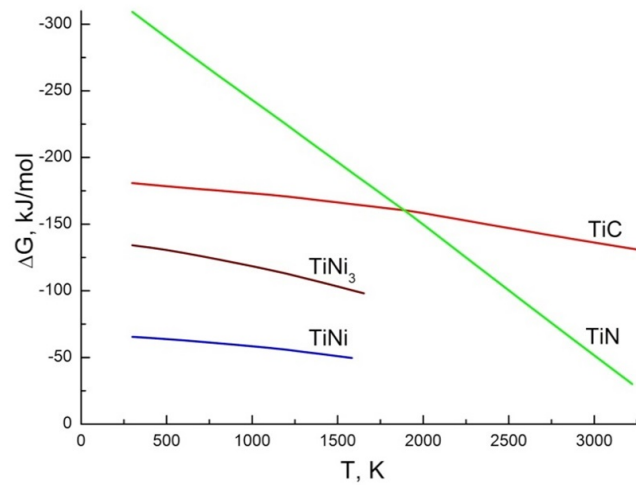


FIG. 5. Dependences $\Delta G(T)$ for compounds TiC, TiN, TiNi₃, TiNi

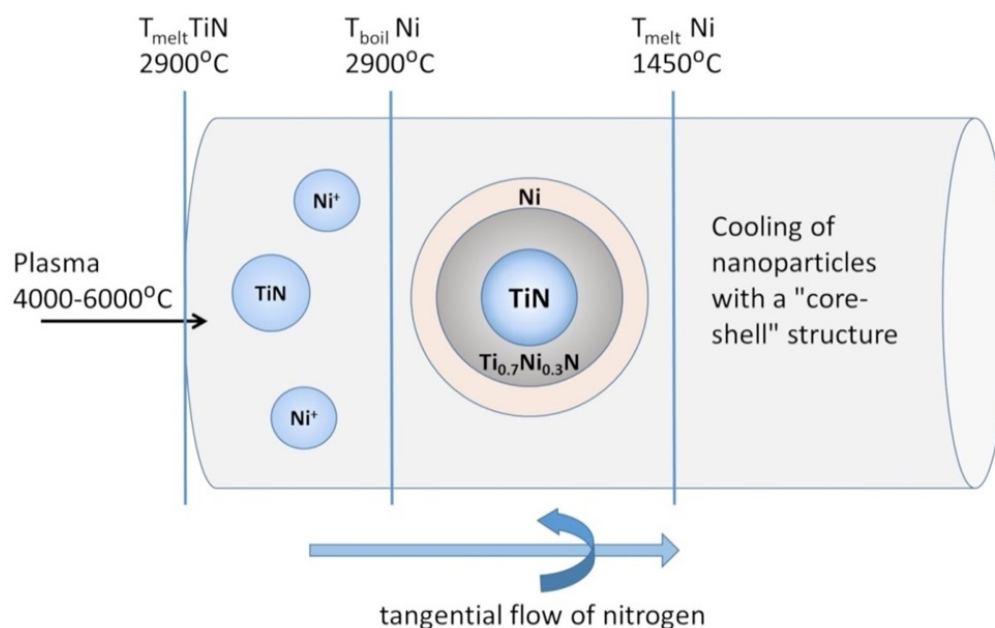


FIG. 6. Chemical mechanism of formation of TiN-Ni “core-shell” structures

nonstoichiometric state of refractory interstitial phases based on titanium, despite the presence of a sufficient amount of gaseous nitrogen, is governed by high crystallization rates under the conditions of the quenching chamber. Nickel metal at these stages is initially in the gaseous state and under these conditions does not react with gaseous nitrogen to form nickel nitrides. Nickel can partially react with gaseous titanium giving rise to Ti–Ni intermetallic compounds (Table 1, experiment 1). At 29–13°C (Table 2), gaseous Ni passes to a liquid phase, which allows intensive interaction with refractory titanium compounds. The fraction from the bag-type filter contains the complex titanium-nickel nitride $\text{Ti}_{0.7}\text{Ni}_{0.3}\text{N}$, which is supposed to be formed in the process of interaction between solid-phase titanium nitride $\text{TiN}_{0.7}$ and liquid Ni at a temperature of 1600°C [22] according to reaction.



A further decrease in temperature is responsible for the crystallization of metallic Ni on the surface of ultra- and nanodispersed particles and their cooling.

Pneumatic transport under the conditions of the plasma-chemical plant provides the transfer of all crystallized particles to the vortex-type cyclone, where the heavier, due to the presence of a larger number of phases (Table 1), ultrafine fraction is separated from the lighter nanocrystalline fraction. The nanocrystalline fraction is concentrated in the bag-type filter. The mechanism of formation of ultra- and nanodispersed “core-shell” structures is shown schematically in Fig. 6.

4. Conclusion

Based on the results of the research performed, it should be noted in conclusion that ultrafine and nanocrystalline TiN-Ni powder fractions with a “core-shell” structure were formed in the process of plasma-chemical synthesis of titanium nickelide in a low-temperature nitrogen plasma. The X-ray diffraction study revealed the phase composition of the powder compositions, in particular, it was shown that the nanocrystalline powder fraction contains the complex titanium-nickel nitride $\text{Ti}_{0.7}\text{Ni}_{0.3}\text{N}$ of hexagonal modification (sp. gr. P-6m2). High-resolution transmission electron microscopy was used to examine the TiN-Ni nanocrystalline fraction, in which the “core-shell” structure was visualized and the presence of all phase components determined by X-ray diffraction, including $\text{Ti}_{0.7}\text{Ni}_{0.3}\text{N}$, was confirmed.

Based on the experimental results obtained and their structural and morphological certification, we have developed a theoretical model of the formation of “core-shell” structures, which shows that the phase and structure formation in the TiN-Ni system depends on the crystallization rate and the presence of a cooling medium in the form of a rotating cylinder of gaseous nitrogen.

References

- [1] Liu F., Yang X., Dang D., Tian X. Engineering of hierarchical and three-dimensional architectures constructed by titanium nitride nanowire assemblies for efficient electrocatalysis. *ChemElectroChem*, 2019, **6**, P. 2208–2214.
- [2] Wang D., Xue C., Cao Y., Zhao J. Microstructure design and preparation of $\text{Al}_2\text{O}_3/\text{TiC}/\text{TiN}$ micro-nano-composite ceramic tool materials based on properties prediction with finite element method. *Ceram. Int.*, 2018, **44**, P. 5093–5101.
- [3] Cui X., Wang D., Guo J. Effects of material microstructure and surface microscopic geometry on the performance of ceramic cutting tools in intermittent turning. *Ceram. Int.*, 2018, **44**, P. 8201–8209.

- [4] Zhang J., Li S., Lu C., Sun C., Pu S., Xue Q., Lin Y., Huang M. Anti-wear titanium carbide coating on low-carbon steel by thermo-reactive diffusion. *Surf. Coat. Technol.*, 2019, **364**, P. 265–272.
- [5] Sarycheva A., Polemi A., Liu Y., Dandekar K., Anasori B., Gogotsi Y. 2D titanium carbide (MXene) for wireless communication. *Science Advances*, 2018, **4**(9).
- [6] Drozdov V.O., Cherepanov A.N., Chesnokov A.E., Smirnov A.V. Studying the production of modifying composite powders by plasma processing. *AIP Conference Proceedings*, 2018, **2053**, 030010.
- [7] Simonenko E.P., Simonenko N.P., Sevastyanov V.G., Kuznetsov N.T. ZrB₂/HfB₂-SiC ceramics modified by refractory carbides: an overview. *Russ. J. Inorg. Chem.*, 2019, **64**, P. 1697–1725.
- [8] Hammouti S., Holybee B., Zhu W., Allain J. P., Jurczyk B., Ruzic D.N. Titanium nitride formation by a dual-stage femtosecond laser process. *Appl. Phys. A*, 2018, **124**, 411.
- [9] Guo W.-P., Mishra R., Cheng C.-W., Wu B.-H., Chen L.-J., Lin M.-T., Gwo S. Titanium nitride epitaxial films as a plasmonic material platform: alternative to gold. *ACS Photonics*, 2019, **6**(8), P. 1848–1854.
- [10] Corradetti S., Carturana M., Maggionia G., Franchin G., Colombo P., Andrighetto A. Nanocrystalline titanium carbide/carbon composites as irradiation targets for isotopes production. *Ceram. Int.*, 2020, **46**(7), P. 9596–9605.
- [11] Huang H., Feng T., Gan Y., Fang M., Xia Y., Liang C., Tao X., Zhang W. TiC/NiO Core/Shell nanoarchitecture with battery-capacitive synchronous lithium storage for high-performance lithium-ion battery. *ACS Appl. Mater. Interfaces*, 2015, **7**(22), P. 11842–11848.
- [12] Zhang Y., Song R., Pei Y., Wen E., Zhao Z. The formation of TiC-NbC core-shell structure in hypereutectic high chromium cast iron leads to significant refinement of primary M7C₃. *J. Alloys Compd.*, 2020, **824**, 153806.
- [13] Dong S., Chen X., Gu L., Zhou X., Wang H., Liu Z., Han P., Yao J., Wang L., Cui G., Chen L. TiN/VN composites with core/shell structure for supercapacitors. *Mater. Res. Bull.*, 2011, **46**(6), P. 835–839.
- [14] Ding X.-Y., Luo L.-M., Huang L.-M., Luo G.-N., Zhu X.-Y., Cheng J.-G., Wu Y.-C. Preparation of TiC/W core-shell structured powders by one-step activation and chemical reduction process. *J. Alloys Compd.*, 2015, **619**(15), P. 704–708.
- [15] Xia M., Yan Q., Xu L., Zhu L., Guo H., Ge C. Synthesis of TiC/W core-shell nanoparticles by precipitate-coating process. *J. Nucl. Mater.*, 2012, **430**(1-3), P. 216–220.
- [16] Chalmers B. *Principles of solidification*. John Wiley and Sons, Springer, New York, Dordrecht, Heidelberg, London, 1964, 319 p.
- [17] Zalite I., Grabis J., Palcevskis E., Herrmann M. Plasma processed nanosized-powders of refractory compounds for obtaining fine-grained advanced ceramics. *IOP Conf. Ser.: Mater. Sci. Eng.*, 2011, **18**, 062024.
- [18] Filkov M., Kolesnikov A. Plasmachemical synthesis of nanopowders in the system Ti(O,C,N) for material structure modification. *Journal of Nanoscience*, 2016, **2016**, 1361436.
- [19] Polak L. Elementary chemical processes and kinetics in a non-equilibrium and quasi-equilibrium plasma. *Pure Appl. Chem.*, 1974, **39**(3), P. 307–342.
- [20] Storozhenko P.A., Guseinov Sh.L., Malashin S.I. Nanodispersed Powders: Synthesis Methods and Practical Applications. *Nanotech. in Russia*, 2009, **4**, P. 262–274.
- [21] Luo H.L., Duwez P.E. Solid solutions of rhodium with copper and nickel. *Journal of the Less-Common Metals*, 1964, **6**, P. 248–249.
- [22] Schönberg N. The tungsten carbide and nickel arsenide structures. *Acta Metall.*, 1954, **2**, P. 427–432.
- [23] Fultz B., Howe J.M. *Transmission electron microscopy and diffractometry of materials*, 3rd ed. Springer, Berlin, Heidelberg, 2008, 758 p.
- [24] Goryczka T., Morawiec H. Structure studies of the R-phase using X-ray diffraction methods. *J. Alloys Compd.*, 2004, **367**, P. 137–141.
- [25] Van Vucht J.H.N. Influence of radius ratio on the structure of intermetallic compounds of the AB₃ type. *Journal of the Less-Common Metals*, 1966, **11**, P. 308–322.
- [26] Kovba L.M., Trunov V.K. *X-ray phase analysis*. MGU, Moscow, 1976, 232 p. (in Russ.)
- [27] Kosolapova T.Ya. *Handbook of high temperature compounds: properties, production, applications*. CRC Press, New York, Washington, Philadelphia, London, 1990, 958 p.
- [28] Hemenger P., Weik H. On the existence of hexagonal nickel. *Acta Crystallogr.*, 1956, **19**, P. 690–691.
- [29] Ermakov A.N., Luzhkova I.V., Avdeeva Yu.A., Murzakaev A.M., Zainulin Yu.G., Dobrinsky E.K. Formation of complex titanium-nickel nitride Ti_{0.7}Ni_{0.3}N in the “core-shell” structure of TiN – Ni. *Int. J. Refract. Met. Hard Mater.*, 2019, **84**, 104996.
- [30] Barin I. *Thermochemical data of pure substances*. Third edition. VCH, Weinheim, New York, Base1, Cambridge, Tokyo, 1995, 2003 p.
- [31] Otsuka K., Shimizu K., Suzuki Yu. *Shape memory alloys*. Ed. Funakubo X. Metallurgiya, Moscow, 1990, 224 p. (In Russ.)
- [32] Gusev A.I. *Nonstoichiometry, disorder, short-range and long-range order in a solid*. FIZMATLIT, Moscow, 2007, 856 p. (In Russ.)
- [33] Samokhin A.V., Polyakov S.N., Alekseev N.V., Astashov A.G., Tsvetkov Yu.V. Simulation of the process of nanopowder synthesis in a jet-type plasma reactor. I. Statement of the problem and verification of the model. *Fizika i khimiya obrabotki materialov*, 2013, **6**, P. 40–46. (In Russ.)
- [34] Samokhin A.V., Polyakov S.N., Alekseev N.V., Astashov A.G., Tsvetkov Yu.V. Simulation of the process of nanopowder synthesis in a jet-type plasma reactor. II. Formation of nanoparticles. *Fizika i khimiya obrabotki materialov*, 2014, **3**, P. 2–17. (In Russ.)
- [35] Shiryayeva L.S., Gorbuzova A.K., Galevsky G.V. Production and application of titanium carbide (assessment, trends, forecasts). *Nauchno-tekhnicheskiye vedomosti Sankt-Peterburgskogo gosudarstvennogo politekhnicheskogo universiteta*, 2014, **2**(195), P. 100–107. (In Russ.)
- [36] Krzhizhanovskiy R.E., Stern Z.Yu. *Thermophysical properties of non-metallic materials (carbides)*. Handbook, Energiya, Leningrad, 1976, 120 p. (In Russ.)

Submitted 12 April 2022; accepted 14 April 2022

Information about the authors:

Yuliya A. Avdeeva – Institute of Solid State Chemistry, Ural Branch, Russian Academy of Sciences, Pervomaiskaya Street, 91, Ekaterinburg, 620990, Russia; y-avdeeva@list.ru

Irina V. Luzhkova – Institute of Solid State Chemistry, Ural Branch, Russian Academy of Sciences, Pervomaiskaya Street, 91, Ekaterinburg, 620990, Russia; key703@yandex.ru

Alexey N. Ermakov – Institute of Solid State Chemistry, Ural Branch, Russian Academy of Sciences, Pervomaiskaya Street, 91, Ekaterinburg, 620990, Russia; ermakovihim@yandex.ru

Conflict of interest: the authors declare no conflict of interest.